Wideband Harmonic Compensation with a Voltage-Source Hybrid Active Power Filter

M. Routimo, M. Salo and H. Tuusa
Department of Electrical Engineering, Power Electronics
Tampere University of Technology
P.O. Box 692, FIN-33101 Tampere, Finland
mikko.routimo@tut.fi

Abstract—**In this paper a voltage-source hybrid active power filter is examined. Wideband harmonic compensation is achieved by improving the active power filter performance with two methods. Filtering of the low order harmonics is improved with a simple computational control delay compensation method applied to the control system, while the high order harmonics are filtered with a small passive high pass filter connected parallel to the active filter. The control system is presented and the system performance examined with measurements at various operating points. The power losses caused by the hybrid filter system are presented and they are compared to the losses of a voltage-source shunt active filter. The benefits of the proposed system can be clearly seen in the results.**

Keywords-active power filter; control; efficiency; hybrid filter;

I. INTRODUCTION

In recent years voltage source active power filters (APFs), have been widely studied and several methods to control them have been proposed e.g. [1] – [5]. A common problem in active filters is their ability to filter only low order harmonics effectively. This is mainly caused by performing the digital control algorithm and sampling the measurement signals, which cause a delay. Because of this, the control is always late and the control system cannot react fast enough to rapid changes in the current reference. Consequently the filtering of higher order harmonics is difficult but also affects the compensation of lower order harmonics.

Methods to improve the performance of the shunt APF (Fig. 1) have been presented in e.g. [6] – [11]. In [6] a predictive current control method is presented. In the method the active filter current reference is predicted based on the data sampled in previous fundamental periods. The method is very effective in steady state operation of the load and the effects of the calculation delay are compensated, but in transient state the system performance deteriorates. In [7] – [9] a passive filter is connected parallel to a shunt APF. The configuration is effective for damping the high-order harmonics, but the problem caused by the control delay persists with low frequencies. In order to improve the filtering of low order harmonics, the filter configuration will be quite big, since the resonance frequency of the passive filter has to be low. A computational control delay compensation method is presented in [10] and [11]. The method is effective for damping the lower order harmonics and it also performs well under transient state of the load. The drawbacks are that the high order harmonics are not filtered effectively and the switching ripple remains in the supply current.

In this paper a method for wideband harmonic compensation is presented. The main circuit configuration of the system is shown in Fig. 2. The system compensates the low order harmonics using a simple computational control delay compensation method [10], [11], while the high order harmonics are filtered with a small passive high pass filter. In the system the whole filtering band of the APF is utilized and

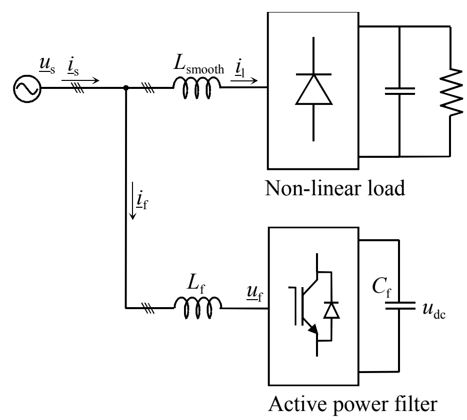

Figure 1. Configuration of the shunt APF

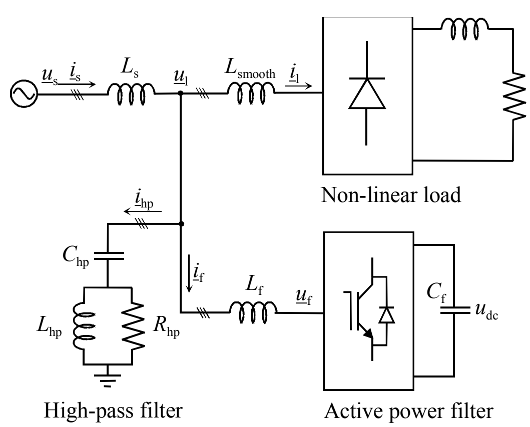

Figure 2. Configuration of the hybrid filter

the filtering performance is recovered with an HPF when the ability of the APF to filter harmonics effectively is impaired. This way the size of the passive filter can be kept small. First the proposed control system is studied. Then the prototype built and the measurement results at various operating points are presented. The results are compared with other filtering methods. Finally power losses in the hybrid filter system are studied and compared to the losses of the voltage-source shunt APF.

II. CONTROL SYSTEM

Fig. 3 presents a block diagram of the proposed control system. Subscripts s, l, f and hp refer to supply, load, active filter and high-pass filter variables respectively, h to harmonics and 0 to fundamental frequency quantities in synchronous reference frame. Underlined variables refer to space vectors, the superscript s to a space vector in synchronously rotating reference frame and * to reference value.

The control system is implemented in the synchronously rotating reference frame, which is tied to the supply voltage vector. The task of the system is to produce a filter current $\underline{i}_{f}$ opposite to the harmonics sensed. The measured load and supply currents, $\underline{i}_{l}$ and $\underline{i}_{s}$ respectively, are first transformed into the synchronously rotating reference frame (blocks "3→2" in Fig. 3). The reference frame angle θ_{s} is determined with a phase locked loop (PLL) by observing supply voltage $\underline{u}_{s}$. Next, the harmonics $\underline{i}^{s}_{lh}$ and $\underline{i}^{s}_{sh}$ are extracted from the fundamental current components with a system based on high-pass filtering (blocks "HP" in Fig. 3). The filter current harmonic reference $\underline{i}^{*s}_{fh}$ is produced with the help of the feedforward of the load currents $\underline{i}_{l}$ and feedback of the supply currents $\underline{i}_{s}$. The feedforward observes harmonics generated by the load and the feedback the harmonics that persist in the supply current after active and passive filtering. The feedback also damps the harmonics drawn by the HPF in the case of distorted supply voltages and prevents resonance.

The effect of the control delay is compensated with the block "CDC" in Fig. 3. The compensation method is based on knowledge of the system dynamics of the APF [10], [11]: since we know the performance of the filter current in case of step change in the current reference, the reference can be corrected so that the filter current behaves as desired. The algorithm can be written in discrete form as

$$\underline{i}^{*s}_{fhl}(k) = -\frac{\tau_c}{T_s}\left(\underline{i}^{s}_{lh}(k) - \underline{i}^{s}_{lh}(k-1)\right) - \underline{i}^{s}_{lh}(k)\,, \tag{1}$$

where τ_c is a compensation time constant and T_s sample time.

The APF dc link voltage is controlled with a fundamental frequency d-axis current reference component i^{*}_{fd0}. This is a dc quantity in synchronous reference frame and is added to the harmonic reference $\underline{i}^{*}_{fh}$. A nonlinear Pe^2 controller is used in voltage control. The controller output is proportional to the square of the input [12]. The reactive power produced by the passive filter is compensated with a fundamental frequency q-axis reference i^{*}_{fq0}. A PID controller is used in the closed-loop control of the filter currents $\underline{i}^{*}_{f}$. Finally the active filter voltage reference $\underline{u}^{*s}_{f}$ is produced by subtracting the filter inductor voltage reference $\underline{u}^{*s}_{Lf}$ from the supply voltage $\underline{u}^{s}_{s}$.

Since the aim in using the HPF is to improve the filtering performance with high order harmonics, the passive filter can be tuned to the frequency where the filtering performance of the active filter is impaired, i.e. close to 1 kHz. The filtering of the harmonics is now divided between the two filters: the APF focuses on the lower order harmonics, while the HPF filters harmonics remaining after active filtering. In conventional shunt APFs the filter inductor inductance L_f is a compromise between current control effectiveness and supply current switching ripple. In the hybrid filter the current control can be further improved by using a smaller filter inductor L_f. In a conventional shunt active filter this would raise the switching ripple in the supply current, but in the hybrid filter the ripple is filtered with the HPF.

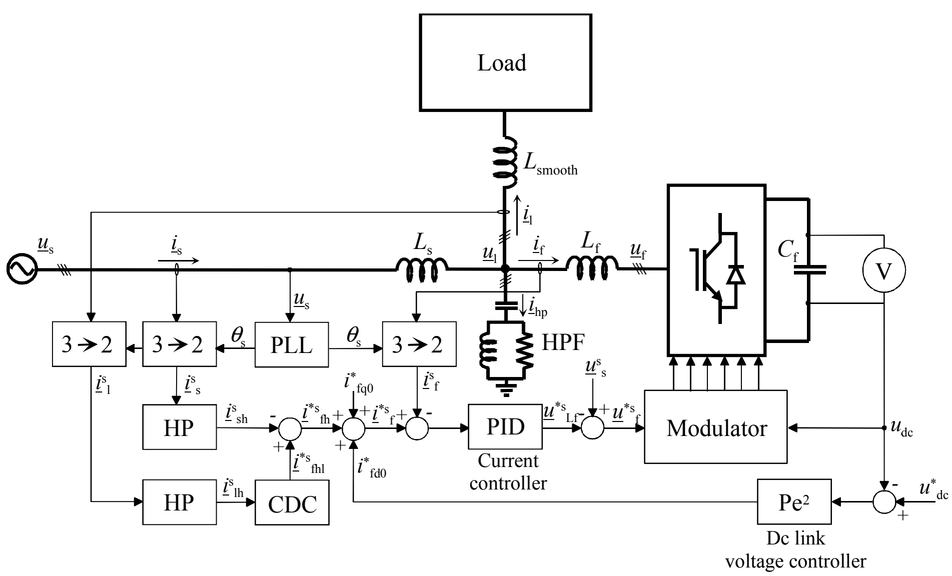

Figure 3. Block diagram of the control system

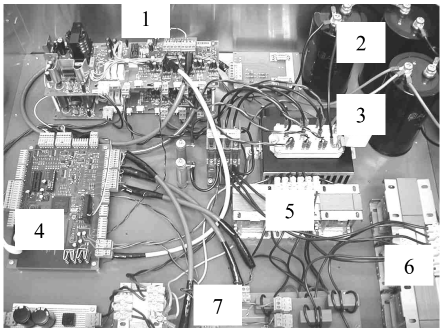

Figure 4. Prototype. 1 drivers, 2 dc link capacitors, 3 IGBT bridge, 4 microcontroller, 5 supply filter L_s, 6 filter inductor L_f, 7 current measuring

TABLE I. HYBRID FILTER PARAMETERS

Supply phase voltage U_s	230 V
Supply frequency f_s	50 Hz
Filter inductor L_f	2.5 mH
Dc-link capacitor C_f	1.1 mF
Smoothing inductor L_{smooth}	2.3 mH
Switching frequency f_{sw}	10 kHz
Passive filter inductor L_{hp}	2.3 mH
Passive filter capacitor C_{hp}	15 µF
Passive filter resistor R_{hp}	3 Ω
Supply filter inductor L_s	1 mH

III. EXPERIMENTAL RESULTS

A. Prototype

The proposed method was tested in the laboratory with an active filter prototype shown in Fig 4. The passive high pass filter is not included in the figure. The prototype has been designed to compensate harmonic currents produced by a nonlinear load of 5 kVA nominal power ($U_{s,LL}$= 400 V). The PWM bridge was built using 1200 V, 40 A IGBTs. The other prototype parameters are shown in Table I. The resonance frequency of the passive high pass filter was chosen to be about 850 Hz.

The control system was implemented using a Motorola MPC555 microcontroller. This is a 32-bit single-chip microcontroller, whose main features are: 448 Kbytes on-chip FLASH EEPROM, 26 Kbytes on-chip RAM, two 8- or 10-bit A/D-converters with 41 input channels each, Modular I/O system (MIOS), two Time Processing Units (TPU) and two Serial Communication Interfaces (SCI), 0.1 µs floating-point multiply and 0.25 µs floating-point divide (at 40 MHz clock frequency).

The time scheduling of the control tasks is based on the interrupts made by the timer unit. The interrupts are generated twice in every modulation period. The modulation frequency is set at 10 kHz, resulting in an interrupt rate of 50 µs. The software procedures are divided into three different priority levels. At the highest level there are protection and time-critical processes like feedforward and closed loop current controls, control delay compensation and the modulator updating. At the second level there is the dc link voltage control that is performed every 75th interrupt time after high priority level tasks. At the lowest priority there are the system synchronization and the user interface updating. These are done at the main program level.

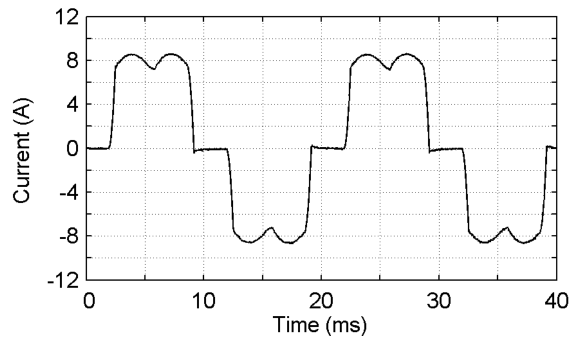

Figure 5. Measured phase-a load current waveform, using a three phase diode bridge supplying an RL load.

B. Measurements

To verify the proposed system filtering performance, two different loads were used in the measurements. First, a diode rectifier that supplied RL load produced the harmonics to be compensated. The load of the diode rectifier consisted of a 10 mH inductance and 64 Ω resistance connected in series. In the other case the harmonic producing load was a diode bridge that supplied an RC load where a 64 Ω resistance was connected in parallel with a 1 mF capacitance. The measured phase-a load current waveform in the case of the RL load is shown in Fig. 5 and the RC load in Figs. 7. The waveforms in Figs. 7a and b are very similar, but there is a slight difference depending on the active filter topology used, to be explained later.

Figs. 6a – d present experimental results with APFs and Table II the harmonic content of the waveforms in the case of the RL load. The active filter dc link voltage reference has been set at 680 V. In Fig. 6a a shunt APF with a conventional, load current feedforward connection based control system [12] has been used. In the case where the control delay compensation method has been applied to the control system of the shunt active filter, the supply current waveform is presented in Fig. 6b [11]. It can be seen in Table II that the method improves the filtering performance of the low order harmonics. In Figs. 6a and b the filter inductor inductance L_f of the shunt APF was 5 mH. The supply current waveform with passive HPF parallel to active filter is presented in Fig. 6c. Now the switching ripple is filtered from the supply current, but clear glitches caused by the control delay can be seen in the waveform. Fig. 6d presents the supply current waveform with the proposed method. With this system the benefits of both the computational control delay compensation method and the shunt active filter with passive HPF are achieved. The system effectively filters harmonics under 2 kHz but also higher frequencies. With the proposed method the total harmonic distortion is reduced from 27.58 % to 2.29 %.

Figs. 7a – b present the measured load current waveforms when the diode bridge supplies an RC load. Fig. 7a corresponds to the situation when the shunt APF is used and Fig. 7b when the hybrid filter is used. Because of the supply inductor in the hybrid filter topology, the active filter operation also affects the voltage $\underline{u}_l$ seen by the load. This reflects on

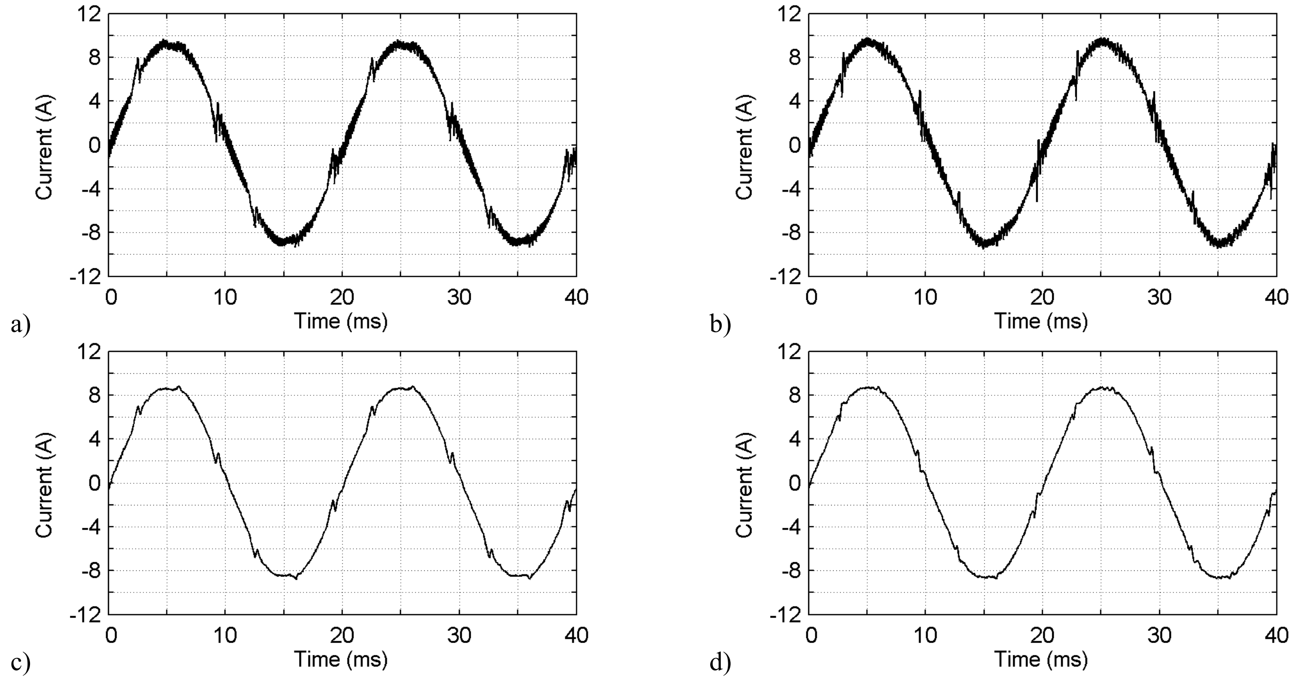

Figure 6. Measured phase-a supply current waveforms in the case of the RL load current presented in Fig. 5, using a) the shunt APF with a conventional control system b) the shunt APF with the control delay compensation method c) the shunt APF with the HPF and d) the proposed method.

TABLE II. HARMONIC CURRENT COMPONENTS

n	RL Load $i_{la(n)}/i_{la(1)}$ [%]	Shunt APF $i_{sa(n)}/i_{sa(1)}$ [%]	Shunt APF with CDC $i_{sa(n)}/i_{sa(1)}$ [%]	Shunt APF with HPF $i_{sa(n)}/i_{sa(1)}$ [%]	Proposed Method $i_{sa(n)}/i_{sa(1)}$ [%]
5	23.07	2.63	1.39	2.19	0.91
7	9.88	1.76	0.71	0.33	0.38
11	7.95	2.24	0.40	1.44	0.07
13	5.21	1.44	0.45	0.60	0.25
17	4.13	1.69	0.60	1.30	0.10
19	3.05	1.33	0.71	0.79	0.24
23	2.27	1.10	0.93	0.88	0.67
25	1.83	1.12	0.85	0.49	0.62
29	1.26	1.01	0.76	0.94	0.82
31	1.10	0.95	0.91	0.51	0.85
35	0.70	0.65	0.56	0.63	0.38
37	0.63	0.60	0.75	0.33	0.58
$THD_{2\ kHz}$	27.55	5.18	2.74	3.58	2.07
$THD_{20\ kHz}$	27.58	6.12	5.91	3.70	2.29

the currents drawn by the diode bridge, since the current drawn by the capacitor depends on the voltages seen by the bridge. This is why the load currents have different harmonic content in Table III. For the active filter to be able to produce compensating currents needed, the dc link voltage is controlled to be 750 V. The supply current waveforms

TABLE III. HARMONIC CURRENT COMPONENTS

n	RC Load $i_{la(n)}/i_{la(1)}$ [%]	Shunt APF with CDC $i_{sa(n)}/i_{sa(1)}$ [%]	RC Load $i_{sa(n)}/i_{sa(1)}$ [%]	Proposed Method $i_{sa(n)}/i_{sa(1)}$ [%]
3	9,22	1,11	5,52	0,58
5	58,31	1,99	56,38	1,07
7	33,00	2,12	30,70	1,22
9	1,89	0,41	1,10	0,04
11	8,46	0,49	7,98	0,18
13	5,13	1,09	4,98	0,83
15	1,29	0,31	0,71	0,05
17	3,05	0,47	2,88	0,11
19	2,29	1,02	2,11	0,94
21	0,94	0,49	0,63	0,15
23	1,94	0,94	2,24	1,09
25	1,38	0,80	1,36	0,96
27	0,71	0,57	0,36	0,41
29	1,23	1,03	1,11	1,39
31	0,83	0,85	0,96	1,37
33	0,50	0,49	0,29	0,56
35	0,78	0,84	0,69	1,63
37	0,62	0,90	0,62	1,45
39	0,41	0,58	0,27	0,88
$THD_{2\ kHz}$	68,57	4,31	65,31	4,07
$THD_{20\ kHz}$	68,58	6,52	65,32	5,05

corresponding to Figs. 7a – b are shown in Figs. 8a – b respectively. The harmonic content of the waveforms is shown in Table III. In Fig. 8a the shunt APF with the control delay compensation method is used and the proposed hybrid filter system is used in Fig. 8b. It can be seen in the table that the load current to be compensated also contains harmonics

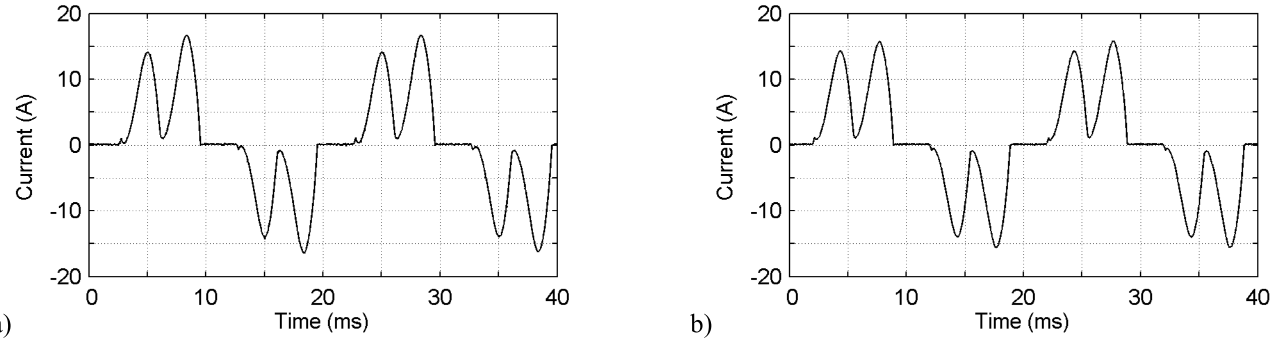

Figure 7. Measured phase-a load current waveforms, using a three phase diode bridge supplying an RC load. a) Shunt APF in operation. b) Hybrid filter in operation

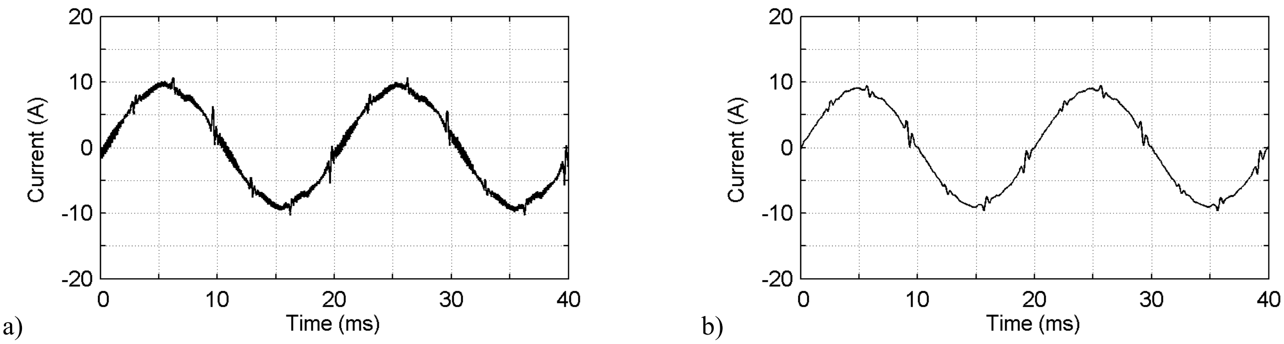

Figure 8. Measured phase-a supply current waveforms in the case of RC load current presented in Fig. 7 using. a) the shunt APF with the control delay compensation method. b) the proposed method.

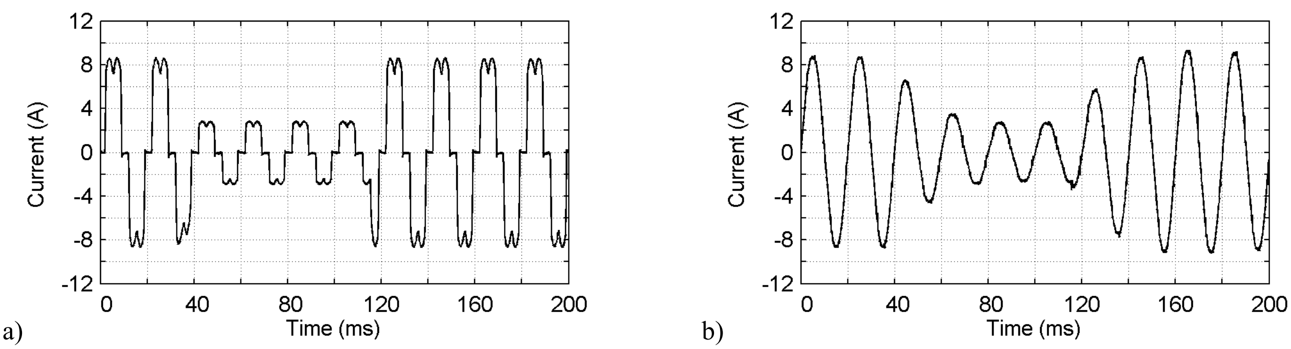

Figure 9. Measured phase-a current waveforms using the proposed method in the case of step chage in the RL load. a) Load current. b) Supply current.

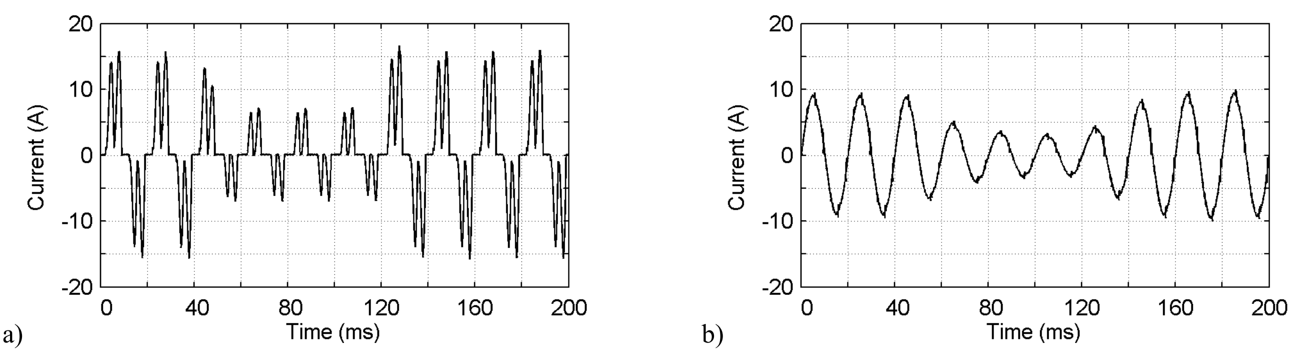

Figure 10. Measured phase-a current waveforms using the proposed method in the case of step chage in the RC load. a) Load current. b) Supply current

of the third order. They are caused by the distorted supply voltages supplying the three phase diode bridge. The fifth and seventh harmonics in the supply voltages give rise to e.g. a third harmonic component in the diode bridge currents. Table III shows that in the supply current $THD_{2\ kHz}$ there is almost no difference between the methods but using the proposed method the $THD_{20\ kHz}$ is about 1.5 percentage units smaller than with the shunt APF.

The performance of the proposed method in the transient state of the load is shown in Figs. 9 – 10. In Figs. 9 an RL type

TABLE IV. FILTER SYSTEM EFFICIENCY

Diode bridge with	RL load		RC load	
	Load power	Filter system	Load power	Filter system
APF + CDC	96,0 %	4,0 %	90,9 %	9,1 %
Proposed Method	95,3 %	4,7 %	90,9 %	9,1 %
Hybrid Filter without Control	99,1 %	0,9 %	99,0 %	1,0 %

load and in Figs. 10 an RC type load is used. In the figures the load resistance changes stepwise from 64 Ω to 193 Ω and back to 64 Ω. As can be seen, the harmonics are also effectively filtered and the supply current is kept sinusoidal under transient state of the load.

C. *Efficiency*

To study the power losses caused by the system examined, power measurements were performed. The aim was to compare the efficiency of the proposed hybrid filter system to the shunt APF controlled using the control delay compensation method. Both systems were controlled so that the power factor of the supply was kept at one. In the measurements the assumption made was that the load is equal in every phase. This why only phase-a supply and load voltages and currents were measured. That is, with the shunt APF the measured quantities were u_{sa}, i_{sa} and i_{la} and with the hybrid filter they were u_{sa}, i_{sa}, u_{la} and i_{la}.

The measurement results are shown in Table IV. Increased compensatory current, when the harmonics of a diode bridge with an RC type load are compensated, causes increase in the power losses of both filter systems. It can be seen in Tables II and III that capacitive type load current has considerably greater harmonics of the orders 3, 5 and 7 than the inductive load type. To compensate them, the active filter has to generate harmonics of equal magnitude. This leads to an increase in the power losses in the filter inductor L_f. The dc link voltage used has also an effect on the increase in power losses in both systems. To compensate the harmonics of the RC type load, the systems used an active filter dc link voltage of 750 V. This is greater than the voltage used in the case of RL type load (680 V). This why switching losses in the IGBT bridge increase.

Table IV demonstrates that even the hybrid filter is a more complicated system with more components, it has almost the same efficiency as the conventional shunt active filter. When the harmonics of the diode bridge with the RL load are compensated, the shunt active filter has slightly lower losses than the hybrid filter, but with the RC type load the efficiencies of the systems are equal. Although the power losses are the same as in the shunt APF, the hybrid filter achieves better filtering result, as can be seen in Table III. With the RL load the efficiency of the hybrid system is lower, but it has a better overall harmonic filtering (Table II).

IV. CONCLUSIONS

In this paper a method to achieve wideband harmonic compensation with a voltage-source hybrid active power filter was presented. The proposed method combines two methods to improve the performance of the shunt active filter: the computational control delay compensation was used to improve the filtering with low order harmonics while the higher frequencies were filtered with a passive high pass filter. The passive filter size was kept quite small, utilizing the whole filtering band of the active filter and tuning the passive filter resonance frequency where the active filter performance is degraded. The hybrid filter performance was examined with different kinds of load through measurements on a prototype in a laboratory and the results were compared to other filtering methods. The results prove the effectiveness of the proposed system for filtering the harmonics. The efficiency of the proposed system was compared to the shunt active filter and it was seen that there is only a small difference when harmonics of an RL type load are compensated, but with an RC type load the efficiencies are equal.

REFERENCES

[1] Akagi, H., "New Trends in Active Filters for Power Conditioning," IEEE Transactions on Industry Applications, vol. 32, no. 6, pp. 1312 – 1322, Nov.-Dec. 1996.

[2] N. Mendalek, K. Al-Haddad, "Modeling and nonlinear control of shunt active power filter in the synchronous reference frame," in Proc. 9th International Conference on Harmonics and Quality of Power, ICHQP, 2000, Orlando, USA, vol. 1, pp. 30 – 35.

[3] N. Mendalek, K. Al-Haddad, L. A. Dessaint, F. Fnaiech, "Nonlinear control strategy applied to a shunt active power filter," in Proc. IEEE 32nd Annual Power Electronics Specialists Conference, PESC, 2001, Vancouver, Canada, vol. 4, pp. 1877 – 1882.

[4] A. Chandra, B. Singh, B. N. Singh, K. Al-Haddad, "An improved control algorithm of shunt active filter for voltage regulation, harmonic elimination, power-factor correction, and balancing of nonlinear loads," IEEE Transactions on Power Electronics, vol. 15, no. 3, pp. 495 – 507, May 2000.

[5] P. Mattavelli, "A closed-loop selective harmonic compensation for active filters," IEEE Transactions on Industry Applications, vol. 37, no. 1, pp. 81-89, Jan.-Feb. 2001.

[6] S. Mariethoz, A. C. Rufer, "Open loop and closed loop spectral frequency active filtering," IEEE Transactions on Power Electronics, vol. 17, no. 4, pp. 564 – 573, Jul. 2002.

[7] S. Fukuda, T. Endoh, "Control method and characteristics of active power filters," in Proc. 5th European Conference on Power Electronics and Applications, EPE, 1993, Brighton, UK, vol. 8, pp. 139 – 144.

[8] S. Fukuda, T. Endoh, "Control method for a combined active filter system employing a current source converter and a high pass filter," IEEE Transactions on Industry Applications, vol. 31, no. 3, pp. 590 – 597, May-Jun. 1995.

[9] S. Khositkasame, S. Sangwongwanich, S., "Design of harmonic current detector and stability analysis of a hybrid parallel active filter," in Proc. Power Conversion Conference, PCC, 1997, Nagaoka, Japan, vol. 1, pp. 181 – 186.

[10] M. Salo, H. Tuusa, "A novel open-loop control method for a current-source active power filter," IEEE Transactions on Industrial Electronics, vol. 50, no. 2, pp. 313 – 321, Apr. 2003.

[11] M. Routimo, M. Salo, H. Tuusa, "A control delay compensation method for voltage source active power filter," in Proc. 9th European Power Quality Conference, PCIM 2003 Europe, Nürnberg, Germany, pp. 93 – 97.

[12] M. Routimo, M. Salo, H. Tuusa, "Experimental results of a voltage source shunt active power filter," in Proc. Nordic Workshop on Power and Industrial Electronics, NORPIE, Stockholm, Sweden, 2002, CD-ROM, 6 p.